

Nanofiber Fractionalization Stimulates Healing of Large Intestine Anastomoses in Rabbits

Martin Kralovic^{1,2}, Michal Vjaclovsky³, Zbynek Tonar⁴, Martina Grajciarova⁴, Jana Lorenzova⁵, Martin Otahal⁶, Alois Necas⁵, Jiri Hoch^{3,7}, Evzen Amler^{1,2}

¹Quality of Indoor Environment, University Centre for Energy Efficient Buildings, Czech Technical University in Prague, Buzehrad, Czech Republic; ²Department of Biophysics, Second Medical Faculty, Charles University in Prague, Prague, Czech Republic; ³Department of Surgery, Motol University Hospital, Prague, Czech Republic; ⁴Department of Histology and Embryology and Biomedical Centre, Faculty of Medicine in Pilsen, Charles University, Prague, Czech Republic; ⁵Section of Small Animal Diseases, Faculty of Veterinary Medicine, University of Veterinary Sciences Brno, Brno, Czech Republic; ⁶Department of Natural Sciences, Faculty of Biomedical Engineering in Kladno, Czech Technical University in Prague, Prague, Czech Republic; ⁷Department of Surgery, Second Medical Faculty, Charles University in Prague, Prague, Czech Republic

Correspondence: Martin Kralovic, Quality of Indoor Environment, University Centre for Energy Efficient Buildings, Czech Technical University in Prague, Trinecka 1024, Buzehrad, 273 43, Czech Republic, Tel +420 224 356 701, Email martin.kralovic@cvut.cz

Background: A current topic of major interest in regenerative medicine is the development of novel materials for accelerated healing of sutures, and nanofibers seem to be suitable materials for this purpose. As various studies have shown, nanofibers are able to partially substitute missing extracellular matrix and to stimulate cell proliferation and differentiation in sutures. Therefore, we tested nanofibrous membranes and cryogenically fractionalized nanofibers as potential materials for support of the healing of intestinal anastomoses in a rabbit model.

Materials and Methods: We compared cryogenically fractionalized chitosan and PVA nanofibers with chitosan and PVA nanofiber membranes designed for intestine anastomosis healing in a rabbit animal model. The anastomoses were biomechanically and histologically tested.

Results: In strong contrast to nanofibrous membranes, the fractionalized nanofibers did show positive effects on the healing of intestinal anastomoses in rabbits. The fractionalized nanofibers were able to reach deep layers that are key to increased mechanical strength of the intestine. Moreover, fractionalized nanofibers led to the formation of collagen-rich 3D tissue significantly exceeding the healing effects of the 2D flat nanofiber membranes. In addition, the fractionalized chitosan nanofibers eliminated peritonitis, significantly stimulated anastomosis healing and led to a higher density of microvessels, in addition to a larger fraction of myofibroblasts and collagen type I and III. Biomechanical tests supported these histological findings.

Conclusion: We concluded that the fractionalized chitosan nanofibers led to accelerated healing for rabbit colorectal anastomoses by the targeted stimulation of collagen-producing cells in the intestine, the smooth muscle cells and the fibroblasts. We believe that the collagen-producing cells were stimulated both directly due to the presence of a biocompatible scaffold providing cell adhesion, and indirectly, by a proper stimulation of immunocytes in the suture.

Keywords: cryogenic grinding, electrospinning, colorectal anastomoses, microvessels, collagen

Introduction

Novel biomaterials designed to enhance tissue regeneration can bring new opportunities to advance the effectiveness of surgical procedures. Surgical procedures have a traumatic effect on microvessels that reduces the blood supply to healed tissues. Sufficient nutrient and oxygen supply is a key factor for collagen synthesis. Resulting shortage of collagen in regenerating tissue leads to weaknesses that could lead to serious postoperative complications.

One of the most serious postoperative complications after an intestinal anastomosis is an anastomotic leak – a defect in the intestinal wall and possible entry point for infection resulting in potential sepsis, multi-organ failure and even death. The most problematic parts of the gastrointestinal tract are the large intestine and the rectum as they have the highest leakage rate, the slowest healing rate and decreased collagen content in healed tissue.¹⁻³ Healed anastomoses

with lowered collagen content have less mechanical strength and are more prone to leakage.⁴ Hence, a potential way to increase the tensile strength of intestinal anastomoses and to reduce leakage rate seems to be to provide support for collagen-producing cells, hence stimulating collagen production.

For cells producing collagen, being adhered to the extracellular matrix (ECM) is vital. Without sufficient cellular adhesion to the ECM, the cells will not be able to proliferate and produce collagen. Therefore, the discontinuity and shortage of ECM at the site of a surgical wound would create a need for a material that would help cells to attach, proliferate and produce further ECM. The material should mimic the structure and functions of ECM. Electrospun nanofibers seem to be a suitable material providing optimal cell adhesion leading to cell proliferation and production of ECM.

However, using electrospun nanofibers for the intestinal anastomoses could have its limitations. Cells perceive electrospun nanofiber mats as a 2D material because the mats do not allow cells to pass through; the cells live only on the surface of the nanofiber mat. However, cells like fibroblasts prefer to be enmeshed in a 3D material that provides more focal adhesions.⁵ Electrospun nanofiber 2D mats are more suitable for superficial placing over skin or fasciae, than for the deeper layers of the intestine that are ultimately responsible for the tensile strength of the intestine. In addition, for manipulation of nanofibers and their attachment to the intestinal surface using stitches, we should prepare mats that are substantial thicker. Over-exposure to polymeric materials may lead to increased immune system reaction and/or chronic foreign body reaction, inflammation and peritonitis, as has been observed in previous studies by our group.

In this study, we compared 2D nanofiber membranes and 3D cryogenically fractionalized nanofibers for healing of the large intestine in rabbits. Fractionized nanofibers enable collagen-producing cells like 3T3 fibroblasts to adhere and proliferate.⁶ We used polyvinyl alcohol and chitosan because the polymers had a proliferative effect on collagen-producing cells *in vitro*.^{7,8} The aim of this study was optimization and regulation of the healing process in anastomosis of the large intestine.

Materials and Methods

Functionalized Nanofibers Preparation, Analysis and Sterilization

Nanofibers were prepared by electrospinning. To obtain purified chitosan, chitosan isolated from shrimp shells was dissolved in a 10% aqueous acetic acid 1% w/v and filtered. The filtered chitosan solution was next precipitated using 1 M NaOH, and the precipitate washed with a mixture of distilled water and acetone and dried at room temperature. Dried purified chitosan was dissolved in a mixture of trifluoroacetic acid (TFA) and dichloromethane (DCM) (7:3 v/v) to obtain 5% w/v chitosan solution.⁹ From the chitosan solution, chitosan nanofibers were prepared with a spinner (MultiSpin, Nanuntio Ltd. Prague, Czech Republic) having a special glass needle electrode and a metal plate collector covered with polypropylene nonwoven textile; the electrical field intensity used was 25 kV/cm. To prevent dissolution of the chitosan nanofibers in the wet environment, the chitosan nanofibers were stabilized in a saturated solution of NaOH in absolute ethanol. After 10 minutes in the NaOH solution, the chitosan nanofibers were washed in distilled water at neutral pH, then dehydrated by immersion in increasing concentrations of ethanol. Dehydrated chitosan nanofibers were dried at room temperature.

Polyvinyl alcohols (5 and 40 kDa, 88% hydrolyzed, Merck) were dissolved in distilled water at 80°C. 12% w/w aqueous PVA solution was used for electrospinning with addition of phosphoric acid to lower the pH and glyoxal as a PVA crosslinker. Electrospinning was performed using a spinner (NanoSpider, Elmarco) with a wire electrode and a wire collector covered with polypropylene non-woven textile; the electrical field intensity used was 25 kV/cm. To prevent dissolution of the chitosan nanofibers in the wet environment, the PVA nanofibers were crosslinked using glyoxal for 72 hours at a temperature of 60°C.

Nanofibers were fractionalized in liquid nitrogen for two working cycles using a cryogenic grinder (Freezer/Mill 6870, SPEX SamplePrep). Each working cycle included 10 grinding (1 min) and re-cooling periods (1 min). The applied impact frequency was 12 Hz.

The morphology of the nanofiber membranes and fractionalized nanofibers was analyzed using scanning electron microscopy (VEGA 3 SBU, Tescan) with a secondary electron (SE) detector at an accelerating voltage of 10 kV. Before

SEM analysis, all samples were sputtered with a thin gold layer using a rotary pumped coater (Q 150R S, Quorum). The average fiber diameter was measured for 100 randomly selected fibers using Tescan software.

We used an accelerated electron beam for sterilization of fractionalized chitosan and PVA nanofibers. Eppendorf vials with ground nanofibers were exposed to an electron beam (9.5 MeV electron energy, 8 μ A electron current and 30 Gy/s absorbed dose rate) on a Microtron MT25 accelerator with a high-frequency source of electrons. During a 15-minute exposure, the dose of radiation used was 27 kGy.

In vivo Experiment

Sixty-two broiler breed Hyplus rabbits (female and male, weight 2.5–3 kg) were obtained from a private breeder. For 10 days before surgery, rabbits were acclimatized, kept at one per cage in standard cages, fed on standard rabbit pellets and water ad libitum. During acclimatization, rabbits were treated with sulfadimidine.

Ethical principles and guidelines for scientific experiments on animals were respected throughout the whole study. The maintenance and handling of the experimental animals followed EU Council Directive 86/609 EEC, and the animals were treated in accordance with the principles of care and use of animals (Decree no. 419/2012 Coll) strictly excluding animal torture. The investigation was approved by the Expert Committee of the Faculty of Veterinary Medicine at the University of Veterinary and Pharmaceutical Sciences, Brno, Czech Republic (protocol number 29–2016) and conformed to Czech Animal Protection Law 246/92.

The rabbits were anesthetized with intramuscularly injected ketamine (50 mg/kg body weight) and xylazine (5 mg/kg body weight) and inhalation of oxygen with 1.5–2% isoflurane. After shaving of the ventral abdominal wall and cleaning with povidone–iodine and chlorhexidine, a 5–6-cm-long midline incision was performed to open the abdominal cavity. The large intestine was transected, then end-to-end anastomosis was manually carried out on the colon, 15 cm from the ileocecal valve using a simple running PDS 4/0 stitch. After stitching of the anastomosis, the suture was powdered with 0.02 grams of ground PVA or chitosan nanofibers. The fascia and skin were closed separately using running stitches. After surgery, rabbits were treated with an intramuscular injection of Ranital (0.2 mL/kg body weight, for 3 days), Degan (0.1 mL/kg body weight, for 3 days), Marbofloxacin (10 mg/kg body weight, one per 24 hours for 7 days) and a subcutaneous injection of Metacam (1 mg/kg body weight, one per 24 hours for 5 days).

Following 14 days from the in vivo experiment, the rabbits were euthanized with an overdose of the intravenous anesthetic thiopental.

Histological Analysis

Thirty rabbits were used for histological analysis in total, 17 samples with no material and 13 samples with material. After euthanasia, 5-cm-long segments of intestine with anastomosis in the middle (marked with stitching material) were resected. The intestinal segments were cut longitudinally, feces were removed and washed with saline solution. The clean segments were fixed in formalin. After formalin fixation, the tissue blocks were processed to 4 μ m-thick histological sections with the section plane parallel to the long axis of the intestine. Each section showed the center of the anastomosis and at least 5 mm of the intestine in both directions.

Two sections were stained with hematoxylin–eosin (for overall morphology of the sample; Bancroft and Stevens, 1996), two with Verhoeff's hematoxylin and green trichrome (to differentiate connective tissue and smooth muscle¹⁰), two with picosirius red (Direct Red 80, Sigma Aldrich, Munich, Germany; to distinguish collagen I and III using polarized light microscopy¹¹), and two with BioGram kit (BioGnost, Zagreb, Croatia; to identify and distinguish Gram-positive and Gram-negative bacteria). Another two sections were immunohistochemically stained to visualize smooth muscle and myofibroblasts (Monoclonal Mouse Anti-Human Smooth Muscle Actin, Clone 1A4, DakoCytomation, Glostrup, Denmark; dilution 1:100); next, two sections to visualize endothelial cells (Monoclonal Anti CD31 antibody Clone J70A, DakoCytomation, Glostrup, Denmark; dilution 1:40) and two last sections for detection of macrophages (Monoclonal Mouse Anti-Human CD68, Clone KP1, DakoCytomation, Glostrup, Denmark; dilution 1:100). Visualization of immunohistochemical reaction was based on diaminobenzidine (DAB+, Liquid; DakoCytomation, Glostrup, Denmark). Immunohistochemical sections were counterstained with Gill's hematoxylin. All sections were dehydrated in graded ethanol solutions and mounted with a xylene-soluble medium.

Four micrographs per each tissue block and staining method were taken using either a 10× objective (α -smooth muscle actin, CD31-positive microvessels) or 20× objective (type I + type III collagen, CD68-positive macrophages) mounted on an Olympus BX41 optical microscope (Olympus, Tokyo, Japan). The image fields were sampled in a systematic uniform random manner as described in detail by Kolinko et al.¹² For picrosirius red microscopy, we used a circular polarizing filter (Hama, Monheim, Germany) crossed with a quarterwave $\lambda/4$ filter below the analyzer filter (U-GAN, Olympus, Tokyo, Japan).

Histological quantification was performed using the stereological point grid¹³ and the following parameters: (i) the volume fraction of the α -smooth muscle actin-positive myofibroblasts within the whole intestinal wall (the smooth muscle of the regular muscular layers of the intestinal wall were not counted in); (ii) the volume fraction of collagen I and III within the whole intestinal wall; (iii) the volume fraction of the CD68-positive cells identified morphologically as macrophages within the whole intestinal wall; (iv) the two-dimensional density of CD31-positive microvessel profiles expressed as the QA (quantity per area) = Q/A , ie, the number of CD31-positive profiles of microvessels (Q) per unit area (A) estimated using an unbiased counting frame.¹⁴ These methods correspond to the approach published recently by Rosendorf et al.¹⁵

As some of the parameters did not pass the Shapiro–Wilk's W -test for normality, nonparametric statistics was used. The Kruskal–Wallis ANOVA followed by the post-hoc Mann–Whitney U -test were used to compare the differences between the Chitosan group, the PVA group, and group of samples without any biomaterial. The correlations among the parameters were assessed using the Spearman correlation coefficient. These tests were used as available in the Statistica Base 11 package (StatSoft, Inc., Tulsa, OK, USA). Significant differences were reported as * $p < 0.05$, ** $p < 0.01$ and *** $p < 0.001$.

Biomechanical Testing

Thirty-two rabbits were used in total, 14 rabbits with no material, 18 rabbits with chitosan. Following rabbits' euthanasia, 5-cm-long intestinal segments with anastomosis in the middle were resected. Feces were removed and washed with saline solution. The clean intestinal segments were placed in saline solution and immediately tested. Biomechanical tests were performed on a MicroTester digital tension meter (a device developed at the Department of Anatomy and Biomechanics, Faculty of Physical Education and Sport, Charles University in Prague, Utility model with document/registration number 25,008, Industrial Property Office, Czech Republic).¹⁶ Throughout the experiment, the structure and tear line of each segment were scanned by an SZX-12 microscope (Olympus, Tokyo, Japan) equipped with an ultrasensitive SensiCam video camera (PCO, Kelheim, Germany). The intestinal segments were individually placed into the jaws of the device in a longitudinal manner and secured. Length, width and thickness were measured for each tested intestinal segment. Next, each fixed intestinal segment was stretched by 5 mm at a speed of 10 mm/s 10 times and then pulled at a speed of 0.5 mm/s until the intestinal segment broke. The tensile response of each sample was recorded throughout the experiment and the yield strength and the maximum tensile strength determined.

Results

Preparation of Implants Based on Functionalized Nanofibers

PVA and chitosan nanofibers were prepared by electrospinning. SEM analysis of the prepared nanofibers showed fibrous morphology (Figure 1A and B). The average diameter of the PVA nanofiber was 324 ± 18 nm. The average diameter of the chitosan nanofibers was 295 ± 97 nm after electrospinning and 314 ± 147 nm after NaOH treatment. Cryogenic fractionation successfully converted the PVA and chitosan and nanofiber membranes into fine powders. The morphology of the powder particles is shown in Figure 1C and D and ranged from submicron-sized fragments of single nanofibers to several micron-sized clusters of nanofibers.

Implantation and Macroscopic Analysis

The application of PVA and chitosan nanofiber membranes onto the anastomoses had disappointing results as they resulted in diarrhea, partial incision dehiscence, presence of abscesses, inflammation and peritonitis and death of animals (Supplementary Figure 1). Moreover, the nanofiber membranes shrunk causing intestinal strictures and obstructions.

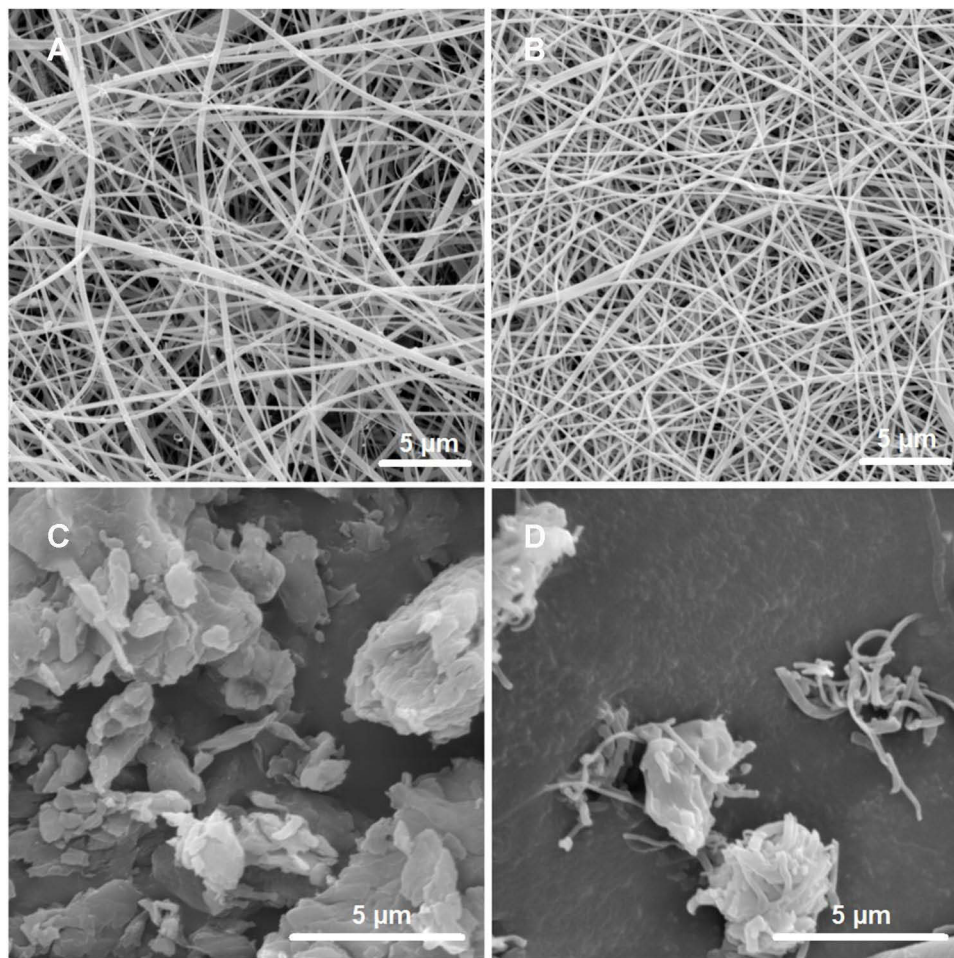


Figure 1 SEM of chitosan (A) and PVA (B) nanofibers, fractionalized chitosan nanofibers (C), and PVA nanofibers (D). Scale bars 5 µm.

By contrast to nanofiber membranes, application of the fractionalized PVA and chitosan nanofibers led to more positive results with respect to the aforementioned issues. No intestinal strictures or intestinal obstructions were observed.

Histological Analysis

Bearing in mind the negative results from the failed application of the nanofiber membranes, we only histologically analyzed the fractionalized nanofibers. The overall histological appearance and the parameters investigated in this study are shown in samples selected randomly from the PVA group, the Chitosan group, and the No Material group in Figure 2. The Gram staining showed only scarce and individually distributed bacteria or their fragments in some of the inflammatory infiltrates.

Quantitative histological analysis showed remarkable differences in the composition of healed anastomoses between the Chitosan, PVA and No Material group (Figure 3). The volume fraction of collagen within the anastomosis wall was greater in samples from the Chitosan group than in the samples from the PVA group (Mann–Whitney $p=0.007$) and the No Material group (Mann–Whitney $p<0.001$). Samples of the PVA and the No Material groups had a comparable volume fraction of collagen within the anastomosis (Mann–Whitney n.s., $p=0.17$).

In a similar way, the volume fraction of actin-positive myofibroblasts within the anastomosis wall was greater in samples from the Chitosan group than in the samples from the No Material group (Mann–Whitney $p=0.003$). There was a tendency towards greater values in samples from the Chitosan group than in the samples from the PVA group, but

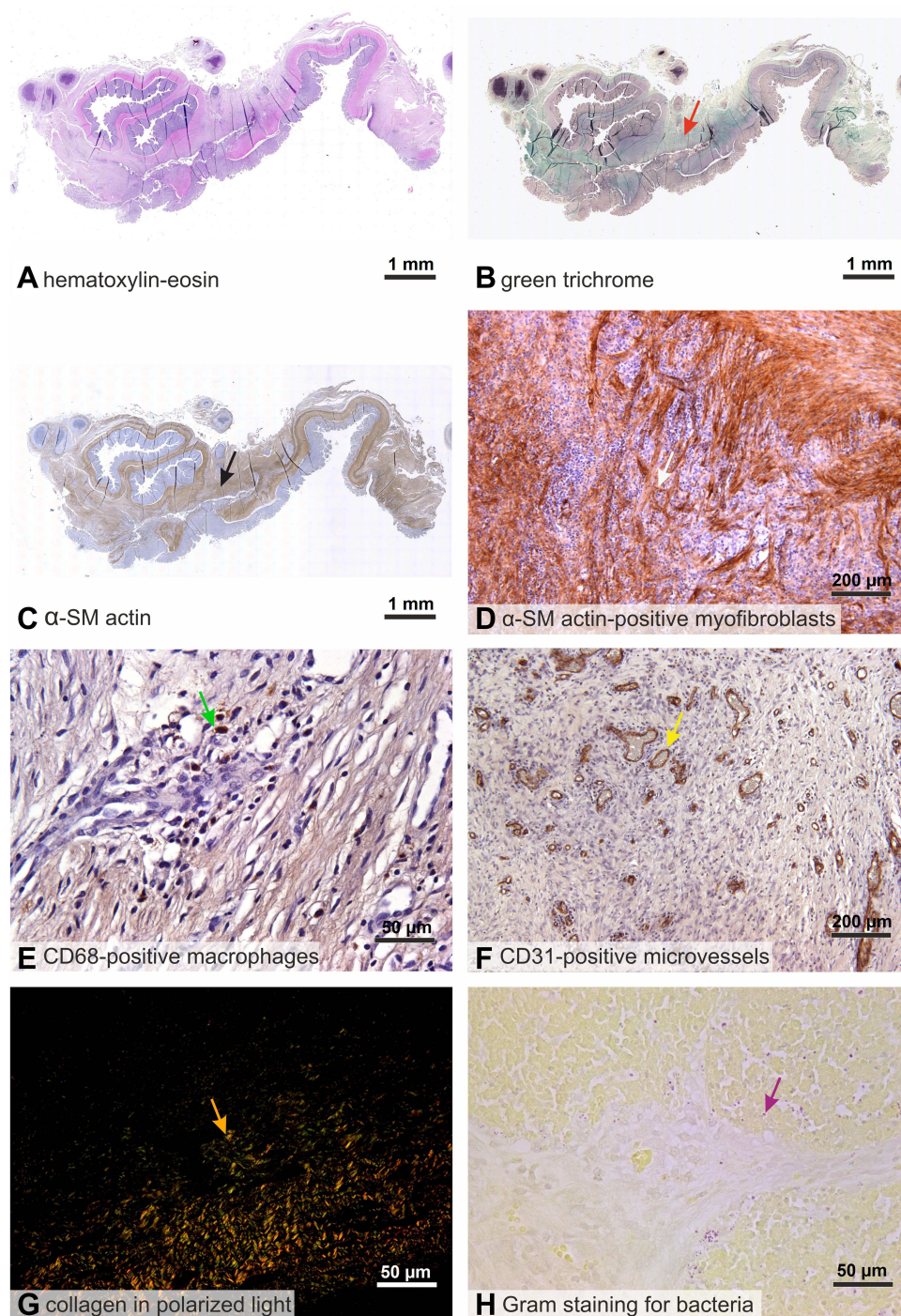


Figure 2 Intestinal anastomoses on longitudinal histological sections stained with various methods. Overall morphology and localization of the anastomosis site were assessed using hematoxylin-eosin staining (**A**). Verhoeff's hematoxylin and green trichrome (**B**) provided a higher contrast picture of the anastomosis, revealing the gap in the muscularis layer (red arrow). This was confirmed using the immunohistochemical reaction against α -smooth muscle actin (**C** and **D**). The gap in the muscularis layer (**C**, black arrow) was often partially filled with α -smooth muscle actin-positive myofibroblasts (**D**, white arrow) proliferating into the granulation tissue filling in the healing defect. Scarce CD68-positive macrophages (**E**, green arrow) were found within the healing defects. CD31 immunohistochemistry (**F**) was used to visualize the microvessels (yellow arrow) within the defect. Assessment of collagen was performed in sections stained with picosirius red observed under circularly polarized light (**G**), where collagen I appeared as reddish and yellow extracellular deposits (orange arrow) and collagen III appeared as green deposits. Bacteria were revealed using the Gram stain modified for use in paraffin-embedded sections (**H**). No large accumulations of bacteria were found; only individual mostly Gram-negative bacteria (magenta arrow) were observed. Scale bars 1 mm (**A-C**), 200 μ m (**D** and **F**), 50 μ m (**E**, **G** and **H**).

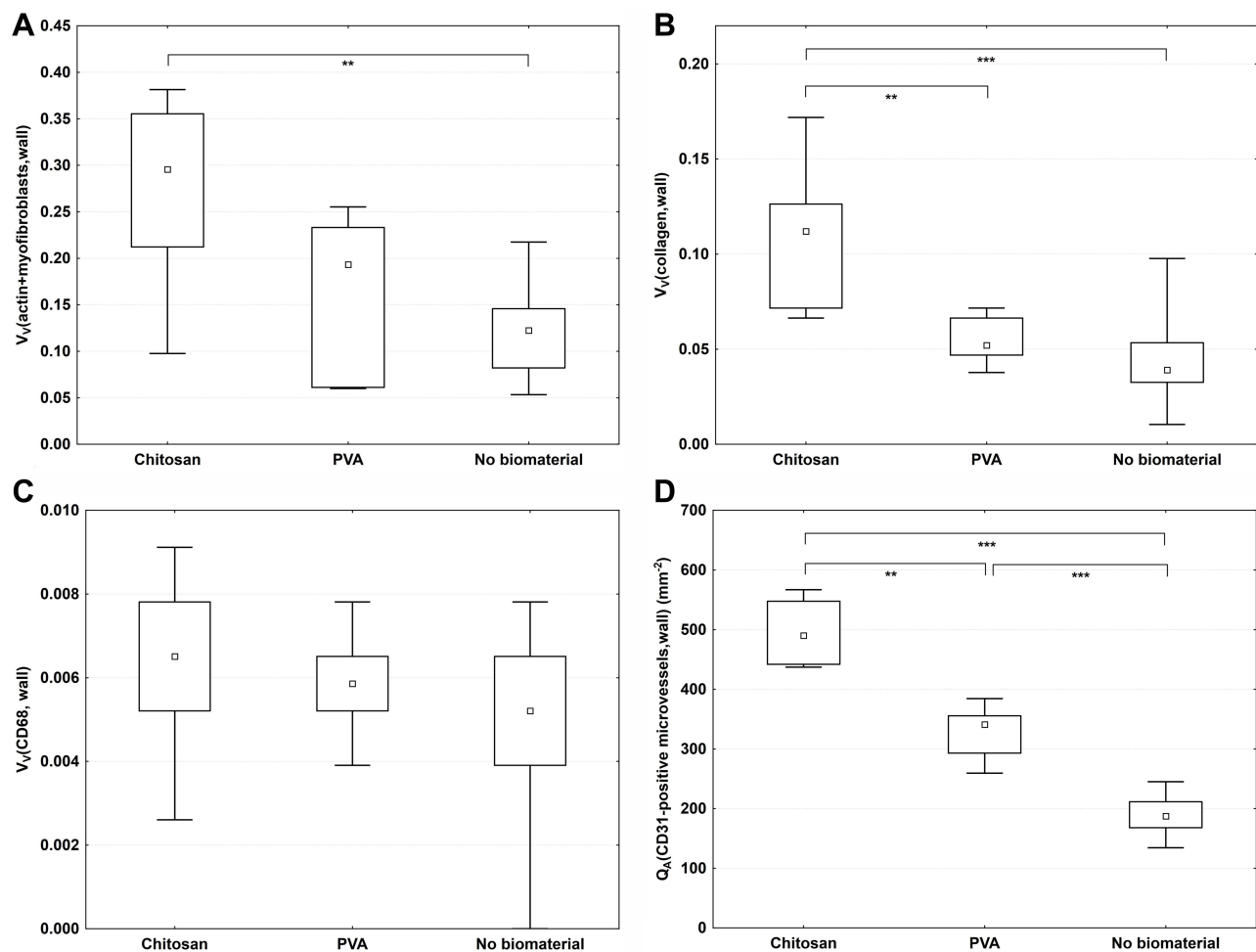


Figure 3 Quantitative histological parameters compared between the experimental groups (Chitosan, PVA and No Material). The anastomoses in the Chitosan group contained a greater fraction of actin-positive myofibroblasts (**A**, Mann–Whitney $p=0.003$) and a greater fraction of collagen (**B**, $p<0.001$) than the No Material group. The anastomoses in the Chitosan group contained a greater fraction of collagen (**B**, $p=0.007$) than the PVA group. The volume fraction of CD68-positive macrophages within the anastomosis did not significantly differ between all groups under study (**C**, Kruskal–Wallis ANOVA n.s., $p=0.16$; post hoc Mann–Whitney tests n.s.). The anastomoses in the Chitosan group contained a greater density of CD31-positive microvessels than the No Material group (**D**, $p<0.001$) and the PVA group (**D**, $p=0.003$). The PVA group differed from the No Material group in containing a greater density of CD31-positive microvessels (**D**, $p<0.001$). Data are displayed as median values (\square , small squares) with boxes spanning the upper limits of the first and third quartiles and with whiskers spanning the minimum and maximum values. V_v refers to the volume fraction of the intestinal wall components at the site of the anastomoses; Q_v refers to the quantity of microvessel profiles per area unit. Significant differences between the groups are indicated as ** $p<0.01$ and *** $p<0.001$.

without statistical significance (Mann–Whitney $p=0.053$). The PVA and the No Material group did not significantly differ in the volume fraction of actin-positive myofibroblasts within the anastomosis wall (Mann–Whitney n.s., $p=0.24$).

The density of CD31-positive microvessels within the anastomosis wall was greater in samples from the Chitosan group than in the samples from the PVA group (Mann–Whitney $p=0.003$) and from the No Material group (Mann–Whitney $p<0.001$). The density was greater in samples from the PVA group than in the samples from the No Material group (Mann–Whitney $p<0.001$).

The volume fraction of CD68-positive macrophages within the anastomosis wall was comparable in all groups under study (Kruskal–Wallis ANOVA n.s., $p=0.16$; post hoc Mann–Whitney tests n.s.).

When pooling all the samples, the density of microvessels was positively correlated with the fraction of myofibroblasts (Spearman $R=0.47$, $p<0.05$), with the fraction of collagen ($R=0.60$, $p<0.05$), as well as with the fraction of macrophages ($R=0.40$, $p<0.05$). These correlations disappeared once these were tested for each group separately.

Biomechanical Analysis

We biomechanically analyzed and compared the control anastomoses (No Material group) to the anastomoses treated with the fractionalized chitosan nanofibers (Chitosan group), chosen as more promising than anastomoses treated with PVA fractionalized nanofibers as our histological analysis had shown.

The intestinal segments with the healed anastomosis in the Chitosan group showed significantly higher values of the ultimate stress than the No Material group. The Chitosan and the No Material groups did not significantly differ in the yield strength. Because native biological structures were measured, the deviation reached high values for both groups as well as for all evaluated parameters.

Values σ_Y , σ_{max} , and E were calculated from the measured data (Table 1). The No Material and the Chitosan groups did not significantly differ in the yield stress (σ_Y) (Mann–Whitney *U*-test, $p=0.755$). Both studied groups differed significantly in the maximum tensile strength (σ_{max}), with high *p*-value (Mann–Whitney *U*-test, $p=0.009$). The Young's modulus (E) was greater in the Chitosan group than in the No Material group ($p=0.007$) (Figure 4).

Based on the evaluated data, it can be deduced that, as was expected, the group in which chitosan had been used was significantly stiffer than the group which had been allowed to heal without the application of any supporting material. What was unexpected was that the yield stress was found to be similar for both procedures. The cause could have been that the intestine had been damaged at the microlevel before the ultimate stress had been reached. This microlevel damage was the same in both groups because it depends only on intestine tissue properties, not on applied healing procedure.

Discussion

Notwithstanding the successful application of nanofiber membranes for acceleration of skin healings,^{17,18} the PVA and chitosan nanofiber membranes caused acute inflammation and peritonitis when applied to the healing of anastomoses of the large intestine. The nanofiber membranes caused acute inflammation and peritonitis. Moreover, shrinkage of the nanofiber membranes during degradation of the materials led to strictures and failures of anastomoses in the rabbits. In another study, placing of the polycaprolactone nanofiber membranes on piglets' anastomoses of the small intestine did not have any stimulating effect on the healing of the anastomoses and nanofiber membranes may have delayed the healing of the anastomoses.¹⁵ Therefore, in general, it does not seem that nanofiber membranes are the optimal solution for the problem of how to effectively support, enhance and accelerate the healing of intestinal anastomoses.

However, successful healing of the large intestinal anastomoses was achieved in our study, when we cryogenically fractionalized both the PVA and the chitosan nanofiber membranes to a fine powder and we scattered the fine powder over the anastomotic wounds. Histological analysis showed significant differences between the healed anastomoses after treatment of the PVA and the fractionalized chitosan nanofibers and the control anastomoses without any material. The anastomoses treated with the fractionized PVA nanofibers had a greater density of microvessels than the control ones. In addition, the anastomoses with the fractionalized chitosan nanofibers had an even denser network of microvessels, more myofibroblasts and more collagen in the healed tissue than the control group. Moreover, in agreement with the histological findings, the biomechanical analysis and higher Young's modulus in the Chitosan group when compared to the No Material group ($p=0.007$) showed mean higher stiffness and lower flexibility which indicated more collagen content in the healed anastomotic tissue.

Table 1 The Values of the Monitored Biomechanical Parameters. (σ_Y , σ_{max} , and E)

Group	Yield Stress (σ_Y) [kPa]	Ultimate Stress (σ_{max}) [kPa]	Young's Modulus (E) [kPa]
No Material	41.251±15.750	50.150±16.849	143.484±55.761
Chitosan	44.319±27.597	74.615±22.126	249.020±98.429

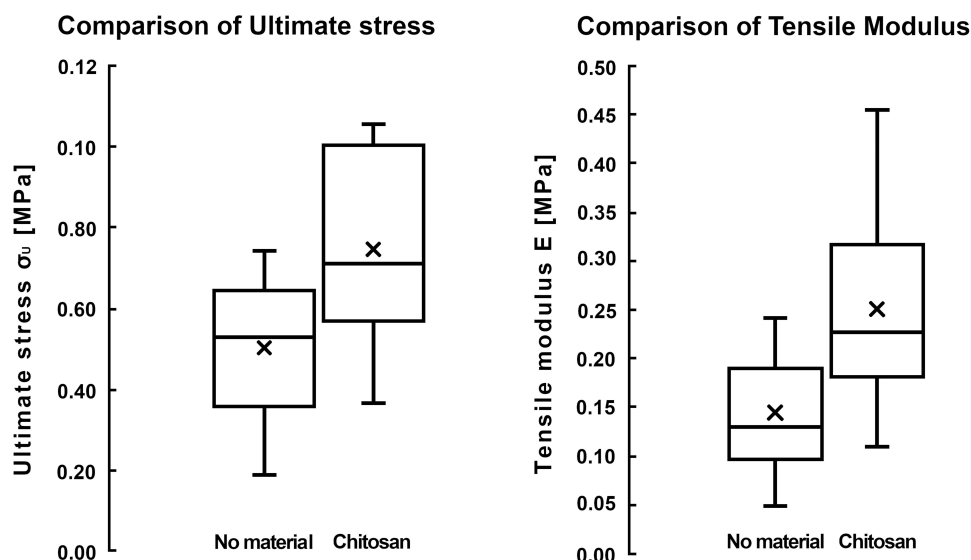


Figure 4 The comparison of the monitored biomechanical parameters. Data are displayed as median values with boxes spanning the upper limits of the first and third quartiles and with whiskers spanning the minimum and maximum values.

The fractionalization of nanofibers apparently increased the biocompatibility of the nanofiber material. The increased surface area and reduced size of the fractionalized nanofibers probably built a better microenvironment for cells in healing anastomosis than a flat nanofiber membrane. Collagen-producing cells like myofibroblasts prefer an environment or a material providing more focal adhesions^{5,19} as in the case of fractionalized nanofibers with increased surface area. Appropriate cell adhesion is a key factor for fibroblast proliferation, differentiation and collagen production. In addition, reduced size of fractionalized nanofibers can be advantageous during the collagen remodelling during the maturation phase of the healing of the anastomosis. Thus, the high versatility of the fractionalized nanofibers due to reduced size of the material do not only hamper maturation of anastomotic wounds but they can accelerate the entire process of anastomosis healing.

Fractionalized chitosan nanofibers can moderately trigger the inflammatory phase of the intestinal anastomoses healing leading to collagen-rich anastomotic tissue. As a naturally occurring compound in the cell wall of parasitic or pathogenic fungi, chitosan triggers immunity response in an animal or the human body. The presence of chitosan in the body activates immunocytes such as neutrophils,²⁰ NK cells and macrophages²¹ that start to produce chitinases, and enzymes able to digest chitosan and break down the fungal cell wall. For macrophage activation in vitro, chitosan must be present in the environment in a soluble form or as particles that macrophages are able to phagocyte.²² In vitro tests showed that submicron sized polymeric particles (800 nm) activate macrophages most effectively.²³ Thus, the fractionalized chitosan nanofibers are ready to be phagocytosed and rapidly activate macrophages in sharp contrast to nanofiber membranes that need to be disintegrated by chitinases from immunocytes before phagocytosis. The larger specific area of the fractionalized chitosan nanofibers could help increase the rate of biodegradation in the macrophages. The activated macrophage release also signals molecules like IL-12, IFN-gamma and TNF-alpha.²² TNF-alpha, an inflammatory cytokine, has proliferative effects on cultured human fibroblasts²⁴ and on the endothelial cells in vivo.²⁵ This is in good agreement with the observed abundant myofibroblasts, collagen fibers and microvessels in the histological sections of the healed anastomoses after treatment by the fractionalized chitosan nanofibers.

Although the volume fraction of CD68-positive macrophages within the anastomosis did not significantly differ between all groups under study, the macrophages in the presence of the fractionalized chitosan nanofibers would be activated. Higher content of the fraction collagen in comparison to the No Material group indicates activation of the collagen-producing cells. The hypothesis should be proven in more detailed future studies.

The described hypothetical pro-inflammatory stimulation is inverse to anti-inflammatory drug delivery via micro-particles that help to reduce the immune response.²⁶ Use of pro- or anti-inflammatory particles depends on the demand

for stimulation of the collagen production. Our pro-inflammatory approach worked towards strengthening of the intestinal anastomoses. However, we assume it would be strongly counterproductive for deep dermal wounds, for avoiding keloids or hypertrophic scars. Our method could find application in general surgery as the agents help strengthen anastomoses in the gastrointestinal tract or the abdominal wall in hernia repair.

Conclusion

Based on the results of the histological analysis, both PVA and fractionalized chitosan nanofibers did exhibit positive effects on the healing of intestinal anastomoses in rabbits. Fractionalized chitosan nanofibers lead to a higher density of microvessels, a greater fraction of myofibroblasts and collagen type I and III than the samples with no material added. Moreover, the fractionalized chitosan nanofibers surpassed the PVA ones in the higher density of microvessels and in the higher amount of collagen. The results of the biomechanical tests supported the histological findings. However, PVA and chitosan nanofibrous membranes did not lead to successfully healed anastomoses. Fractionalization of nanofibers reduced the dose of the materials and the immunity response and stimulated healing of intestinal tissues.

Acknowledgments

The research leading to these results has received funding from the Norway Grants and the Technology Agency of the Czech Republic within the KAPPA Programme FIS: 3122204V000 and the Project FIS: 3122204V000.

Disclosure

The authors report no conflicts of interest in this work.

References

1. Hesp WL, Hendriks T, Schillings PH, et al. Histological features of wound repair: a comparison between experimental ileal and colonic anastomoses. *Br J Exp Pathol*. 1985;66(5):511–518.
2. Pommergaard HC, Gessler B, Burcharth J, et al. Preoperative risk factors for anastomotic leakage after resection for colorectal cancer: a systematic review and meta-analysis. *Colorectal Dis*. 2014;16(9):662–671. doi:10.1111/codi.12618
3. Nordentoft T. Sealing of gastrointestinal anastomoses with fibrin glue coated collagen patch. *Dan Med J*. 2015;62:1–13.
4. Krarup PM, Eld M, Jorgensen LN, et al. Selective matrix metalloproteinase inhibition increases breaking strength and reduces anastomotic leakage in experimentally obstructed colon. *Int J Colorectal Dis*. 2017;32(9):1277–1284. doi:10.1007/s00384-017-2857-x
5. Baker BM, Chen CS. Deconstructing the third dimension—how 3D culture microenvironments alter cellular cues. *J Cell Sci*. 2012;125(Pt 13):3015–3024. doi:10.1242/jcs.079509
6. Knotek P, Pouzar M, Buzgo M, et al. Cryogenic grinding of electrospun poly-ε-caprolactone mesh submerged in liquid media. *Mater Sci Eng C*. 2012;32(6):1366–1374. doi:10.1016/j.msec.2012.04.012
7. Howling GI, Dettmar PW, Goddard PA, et al. The effect of chitin and chitosan on the proliferation of human skin fibroblasts and keratinocytes in vitro. *Biomaterials*. 2001;22(22):2959–2966. doi:10.1016/S0142-9612(01)00042-4
8. Pelipenko J, Kocbek P, Kristl J. Nanofiber diameter as a critical parameter affecting skin cell response. *Eur J Pharm Sci*. 2015;66:29–35. doi:10.1016/j.ejps.2014.09.022
9. Ohkawa K, Minato KI, Kumagai G, et al. Chitosan nanofiber. *Biomacromolecules*. 2006;7(11):3291–3294. doi:10.1021/bm0604395
10. Kocová J. Overall staining of connective tissue and the muscular layer of vessels. *Folia Morphol*. 1970;18(3):293–295.
11. Rich L, Whittaker P. Collagen and picrosirius red staining: a polarized light assessment of fibrillar hue and spatial distribution. *Braz J Morphol Sci*. 2005;22:97–104.
12. Kolinko Y, Malečková A, Kochová P, et al. Using virtual microscopy for the development of sampling strategies in quantitative histology and design-based stereology. *Anat Histol Embryol*. 2022;51(1):3–22. doi:10.1111/ah.12765
13. Mouton PR. *Principles and Practices of Unbiased Stereology. An Introduction for Bioscientists*. Baltimore, MD, USA: Johns Hopkins University Press; 2002.
14. Tonar Z, Egger GF, Witter K, et al. Quantification of microvessels in canine lymph nodes. *Microsc Res Tech*. 2008;71(10):760–772. doi:10.1002/jemt.20619
15. Rosendorf J, Horakova J, Klicova M, et al. Experimental fortification of intestinal anastomoses with nanofibrous materials in a large animal model. *Sci Rep*. 2020;10:1–12.
16. Plencner M, East B, Tonar Z, et al. Abdominal closure reinforcement by using polypropylene mesh functionalized with poly-ε-caprolactone nanofibers and growth factors for prevention of incisional hernia formation. *Int J Nanomedicine*. 2014;9:3263–3277. doi:10.2147/IJN.S63095
17. Tchemtchoua VT, Atanasova G, Aqil A, et al. Development of a chitosan nanofibrillar scaffold for skin repair and regeneration. *Biomacromolecules*. 2011;12(9):3194–3204. doi:10.1021/bm200680q
18. Buzgo M, Plencner M, Rampichova M, et al. Poly-ε-caprolactone and polyvinyl alcohol electrospun wound dressings: adhesion properties and wound management of skin defects in rabbits. *Regen Med*. 2019;14(5):423–445. doi:10.2217/rme-2018-0072
19. Cukierman E, Pankov R, Stevens DR, et al. Taking cell-matrix adhesions to the third dimension. *Science*. 2001;294(5547):1708–1712. doi:10.1126/science.1064829

20. Minami S, Oh-Oka M, Okamoto Y, et al. Chitosan-inducing hemorrhagic pneumonia in dogs. *Carbohydr Polym*. 1996;29(3):241–246. doi:10.1016/0144-8617(95)00157-3
21. Nishimura K, Nishimura S, Nishi N, et al. Immunological activity of chitin and its derivatives. *Vaccine*. 1984;2(1):93–99. doi:10.1016/S0264-410X(98)90039-1
22. Shibata Y, Metzger WJ, Myrvik QN. Chitin particle-induced cell-mediated immunity is inhibited by soluble mannan: mannose receptor-mediated phagocytosis initiates IL-12 production. *J Immunol Res*. 1997;159:2462–2467.
23. Chikaura H, Nakashima Y, Fujiwara Y, et al. Effect of particle size on biological response by human monocyte-derived macrophages. *Biosurf Biotribol*. 2016;2(1):18–25. doi:10.1016/j.bsbt.2016.02.003
24. Battegay EJ, Raines EW, Colbert T, et al. TNF-alpha stimulation of fibroblast proliferation. Dependence on platelet-derived growth factor (PDGF) secretion and alteration of PDGF receptor expression. *J Immunol*. 1995;154(11):6040–6047.
25. Fräter-Schröder M, Risau W, Hallmann R, et al. Tumor necrosis factor type alpha, a potent inhibitor of endothelial cell growth in vitro, is angiogenic in vivo. *Proc Natl Acad Sci USA*. 1987;84(15):5277–5281. doi:10.1073/pnas.84.15.5277
26. Wofford KL, Singh BS, Cullen DK, et al. Biomaterial-mediated reprogramming of monocytes via microparticle phagocytosis for sustained modulation of macrophage phenotype. *Acta Biomater*. 2020;101:237–248. doi:10.1016/j.actbio.2019.11.021

International Journal of Nanomedicine

Dovepress

Publish your work in this journal

The International Journal of Nanomedicine is an international, peer-reviewed journal focusing on the application of nanotechnology in diagnostics, therapeutics, and drug delivery systems throughout the biomedical field. This journal is indexed on PubMed Central, MedLine, CAS, SciSearch®, Current Contents®/Clinical Medicine, Journal Citation Reports/Science Edition, EMBase, Scopus and the Elsevier Bibliographic databases. The manuscript management system is completely online and includes a very quick and fair peer-review system, which is all easy to use. Visit <http://www.dovepress.com/testimonials.php> to read real quotes from published authors.

Submit your manuscript here: <https://www.dovepress.com/international-journal-of-nanomedicine-journal>